Progress In Electromagnetics Research C, Vol. 55, 43–52, 2014

Dual-band Circularly-Polarized Monopulse Antenna System with Single Layer Patches and Separated Feed Networks

Mahdi Fartookzadeh* and Seyed H. Mohseni Armaki

Abstract—This paper introduces a new method for the design and realization of two monopulse antennas with circular polarization and unique phase center for two different frequency bands. The design uses a compact sequential-rotation serially fed 2×2 patch array for each section of the monopulse antenna for X band at 8.2 GHz and a patch for S band at 2.25 GHz. The patches are placed on one layer, and the monopulse network and feeds are placed on different layers. The antennas use sequential-rotation serial feeds with four and three probes for X band and S band, respectively. Also, the packaging and coupling effects are considered and compensated for this design. Finally, the antenna with a compact multi-layer structure is fabricated, and the simulation results are validated. The bandwidth of X band monopulse antenna system is at least 12.7% in simulation and 10% in fabrication, and it is about 10.2% and 10.3% for S band in simulation and fabrication, respectively. While the phase centers of both frequency bands are approximately at one point, the antenna system can be employed as a feed for reflectors.

1. INTRODUCTION

Earth stations, radar systems, and other direction finders usually need auto-track system to find the accurate angle of the incoming wave. Monopulse tracking system is a well-known auto-track technique that gives a fast and accurate response [1]. It is known that the antenna system consists of feed lines, 90° hybrids or 180° hybrids and antenna elements. The enhancement on the components of the monopulse antenna and comparator is an area of interest for many new records. For example, 180° hybrids based on the Wilkinson power divider and Gysel power divider are introduced respectively in [2] and [3] to obtain a suitable structure for constructing monopulse comparator network. Other examples are the dual-band rat-race coupler that uses a dual-band 180° phase shifter in place of a simple line [4] and the complete monopulse comparator network with four rat-race hybrids in [5].

Complete monopulse antenna and comparator network with linear polarization (LP) are also presented in many recent reports such as [6] and [7] with single-layer array and slot antenna array on substrate integrated waveguide (SIW), respectively. In addition, circularly polarized monopulse antennas are studied in some recent papers using SIW slot array antennas [8], radial line slot antennas [9] and dual-band dielectric rod antennas [10]. Nevertheless, the design of an antenna with circular polarization is a classic topic and the improvement is still a frequent subject. For example, one technique is the employment of multilayer substrate with different structures on each layer [11–14]. The axial ratio (AR) bandwidth (BW) of multilayer structures can be improved if the layers are separated with air or foam layer, and one or more probes are used between the layers [15, 16]. As can be found in [16–19], circular shape usually produces better results for the circular polarization (CP).

It is known that a very useful technique for improvement of the axial ratio bandwidth of antenna arrays is to match the angular and phase arrangements of the elements and use the sequential-rotated

Received 6 October 2014, Accepted 6 November 2014, Scheduled 20 November 2014
* Corresponding author: Mahdi Fartookzadeh (mahdi.fartookzadeh@gmail.com).
The authors are with the Department of Electrical and Electronics Engineering, Malek Ashtar University, Tehran, Iran.

array [20, 21]. The combination of this method with others improves the performance considerably [22–30]. A new technique is a serially fed sequentially rotated antenna array used for one multi-feed antenna in [31] as a shorted-annular-ring reduced-surface-wave patch antenna and in [32] as a three-probe-fed circular patch antenna suitable for arrays. This antenna is also used in this paper, for the monopulse system.

This paper proposes a monopulse antenna and comparator network with right-handed circular polarization (RHCP) for two frequency bands. Two sets are separately designed and placed so that the phase centers of both are located approximately on a point to make it useful as the reflector feeder. While the antennas are separately designed, and the restrictive design methods for dual band antennas are not used, this design can be generalized for any two frequency bands with enough distance.

The components of the monopulse antenna are introduced in the next section. The structure uses 3 substrates with 6 metal layers. Two substrates are for the monopulse comparator of each frequency band, and the antennas are placed on the front layer of the other substrate. The detailed explanation is given in the third section.

2. MONOPULSE ANTENNA AND COMPARATOR COMPONENTS

2.1. Feed Network

The monopulse network is constructed using simple circular 90° hybrids as shown in Fig. 1(a) for the X band. The only difference with the normal square type 90° hybrid is the 90° physical angle between feed lines, which makes the construction of a total network easier as shown in Fig. 2. The phase difference and reflection coefficient are shown in Fig. 1(b), and transmission and isolation are shown in Fig. 1(c). The desired frequency for the X band antenna is 8.2 GHz, and the wide bandwidth improves the signal quality. This hybrid has the $90 \pm 0.3°$ phase difference between S_{13} and S_{14} further than 7.7 GHz in the simulation. Also the amplitude difference does not exceed 0.5 dB after 7.8 GHz, and the isolation and reflection are fine throughout the bandwidth.

The monopulse comparator is composed of four 90° hybrids as shown in Fig. 2. As can be calculated explicitly that if all the antennas had a same geometrical angle, $P3$, $P4$ and $P1$ were the sum, azimuth and elevation differences outputs, respectively. However, it is shown that the geometrical angle for $A3$ and $A4$ are assumed to be 180°; therefore $P1$, $P2$ and $P3$ are the sum, azimuth and elevation differences outputs, respectively. It can be obtained by replacing $L_1 + \lambda_0/4$ by $L_1 - \lambda_0/4$ on the feed-lines of $A3$ and $A4$.

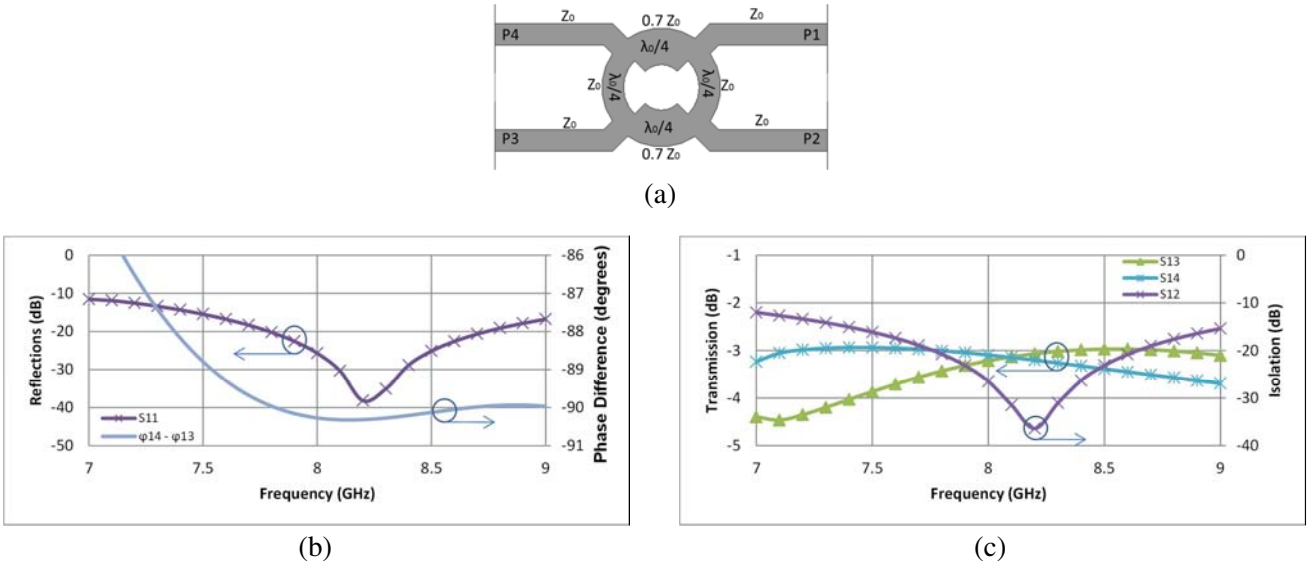

Figure 1. Circular 90° hybrid for X band, (a) schematic, and simulation results (HFSS): (b) reflection and phase difference, (c) transmissions and isolation.

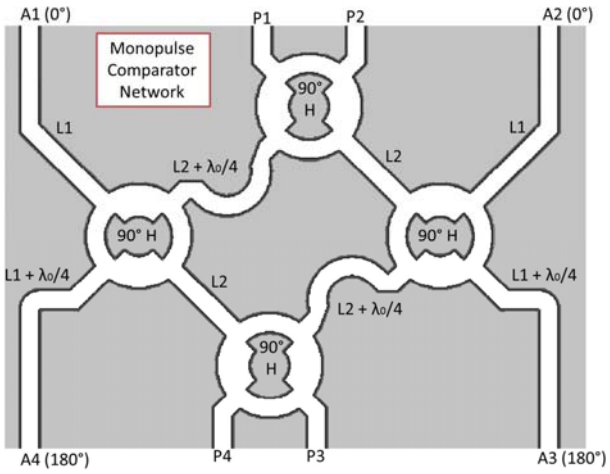

Figure 2. The monopulse comparator network for both frequency bands.

The widths of input and output lines are 1.94 mm on the substrate with $h = 0.762$ mm and $\epsilon_r = 2.55$, which bring in 50 Ω impedances at X band. The desired frequency for the S band antenna is 2.25 GHz, and the same monopulse network with same 90° hybrids is used for the S band. The widths of input and output lines are 6.28 mm ($h = 1.524$ mm and $\epsilon_r = 2.55$), and Z_0 is also about 50 Ω for this frequency band.

2.2. Antenna Elements

A circular patch with four probes of 3.5 mm diameter is used for each quarter of S band antenna as shown in Fig. 3(a). The probes are serially fed with 90° geometrical and electrical angle. For each quarter of X band antenna, a 2×2 array of circular patches with three probes of 1 mm diameter is used as shown in Fig. 3(b). These arrays should be placed between the sections of the S band antenna and should be as compact as possible; hence the sequentially rotated serial feed is used. Radii of the patches are not the same and obtained during optimization for symmetric pattern and best axial ratio bandwidth. The consequent monopulse antenna and network arrangement for X band is shown in Fig. 3(c). Feed lines and comparator network are on the back layer, and the patches are on the front layer, as will be explained in next section.

The difference between the numbers of probes for X band antennas and S band antennas is due to the difference between the widths of substrates of feed lines of the two antennas. It is observed empirically that four probes give better response for the S band antenna while the substrate width of the S band feed line is about half of the X band substrate width proportional to the wavelength.

The input impedance of the probes (Z_p) is dependent on the position and size of them and top layer patch while the impedances of lines between probes (Z_i) are dependent on the width of them and the permittivity and height of substrate, explicitly. For impedance matching of the sequentially-rotated serial-feed-line with N probes, there are infinite solutions for $Z_i s$ and Z_p, with $i = 1, 2, 3, \ldots, N-1$ and $N > 2$, since only one complex equation should be met for lossless lines:

$$Z_0 = Z_{in}^{(1)} = Z_{in}^{'(2)} || Z_p = \frac{Z_1 Z_p \left(Z_{in}^{(2)} + j Z_1 \tan \dfrac{2\pi}{N} \right)}{Z_1 \left(Z_p + Z_{in}^{(2)} \right) + j \left[(Z_1)^2 + Z_{in}^{(2)} Z_p \right] \tan \dfrac{2\pi}{N}}, \tag{1}$$

with

$$Z_{in}^{(i)} = \frac{Z_i Z_p \left(Z_{in}^{(i+1)} + j Z_i \tan \dfrac{2\pi}{N} \right)}{Z_i \left(Z_p + Z_{in}^{(i+1)} \right) + j \left[(Z_i)^2 + Z_{in}^{(i+1)} Z_p \right] \tan \dfrac{2\pi}{N}}$$

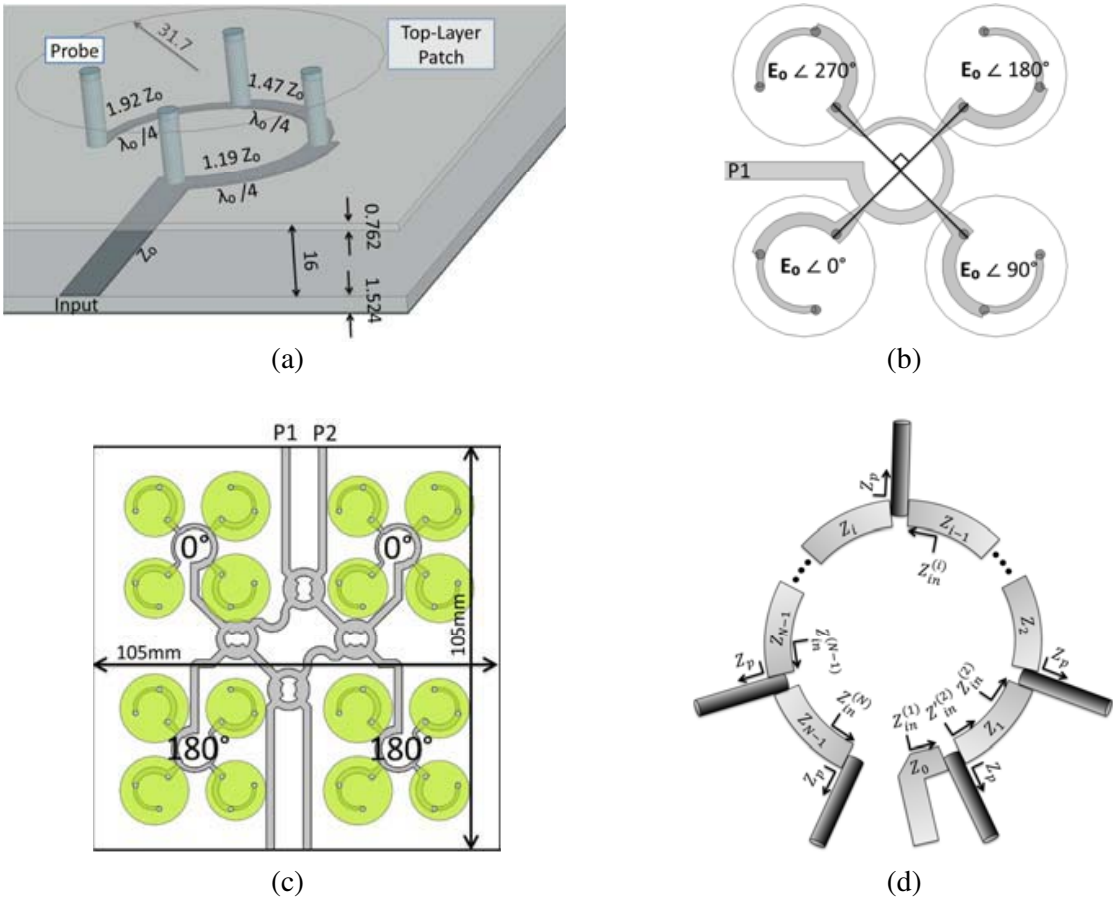

Figure 3. Antenna sections for both frequency bands, (a) single antenna with 4 probes for S band and (b) antenna array with 4 sequentially rotated elements for X band, (c) monopulse antenna and network arrangement for X band, (d) sequentially-rotated serial-feed-line with N probes.

and $Z_{in}^{(N)} = Z_p$ (see Fig. 3(d)).

A simple solution with no reflections is given in [32], and it is explained that the impedance matching is not the only requirement while the power delivered by each probe should be akin with the others. Therefore, we should have $|Z_{in}^{(i)}| = Z_p/(N+1-i)$ for lossless lines. These equations give approximate values for the impedances in a single frequency. Anyway, there are some losses for the lines. Z_p is unknown, and wideband matching is required. Therefore, a combination of this method and simulation optimization produces best results for the impedances of lines. The resulting impedances for the antenna with four probes are shown in Fig. 3(a) with optimization on the axial ratio bandwidth.

3. MONOPULSE ANTENNA AND COMPARATOR TOTAL ARRANGEMENT

The consequent design with three substrates has six metal layers named $L1$ to $L6$ in Fig. 4(a), and the antennas and feed lines for X band are shown in Fig. 4(b). Antenna patches are placed on $L1$ which is the top layer of the front substrate. Major parts of the next layer, $L2$, which is the metal layer behind the front substrate, are removed to allow the connections between feed-lines and patches. There are only two rectangular planes on $L2$ over the X band output lines to block radiation of them. These lines are placed on $L3$ that is the top layer of the middle substrate. They are extended to reach the box sides, and thus they can affect the circular polarization without being blocked by the $L2$ planes. Also the monopulse comparator of X band and the feed networks are placed on $L3$. The feed lines are connected to the small patches of $L1$ with 1 mm probes. In the same way, the monopulse comparator

and the feed network of S band are placed on $L5$ that is the top layer of the behind substrate. The S band feed lines are connected from $L5$ to the large patches of $L1$ with 3.5 mm probes. Finally, the ground planes of the two frequency bands are shown as $L4$ and $L6$.

Therefore, there are three substrates with 2.55 relative permittivity and 0.0015 dielectric loss tangent. The thickness of back substrate, between $L5$ and $L6$, is 1.524 mm. The thickness of middle substrate, between $L3$ and $L4$, is 0.762 mm, and the thickness of front substrate, between $L1$ and $L2$, is also 0.762 mm. It can be seen that the surface of the middle substrate is $105 \times 270\,\text{mm}^2$, and the other substrates are $270 \times 270\,\text{mm}^2$.

While the distance between the box sides and X band ground plane to the S band antenna is much less than the wavelength of the S band, and the coupling effect is important for this frequency band. Therefore, a copper sheet is connected to the surrounding metal box parallel with the substrates to compensate the coupling effect of the X band ground plane. The small side of copper sheet determines the aperture size between the S band feed lines and the patches. Hence, it should not widely differ from 50 mm as shown in Fig. 4 to prevent the frequency band from significant shifting.

Simulation results of the consequent antenna are indicated in Fig. 5(a). It can be observed that the

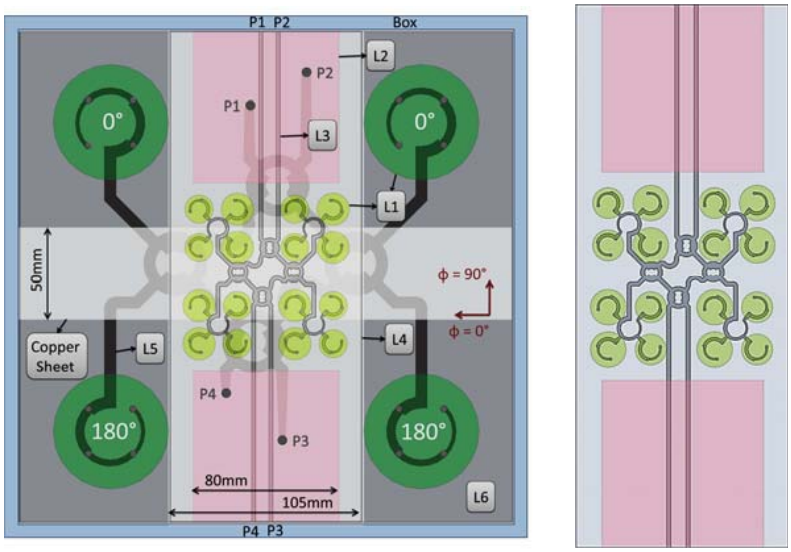

(a) (b)

Figure 4. (a) The proposed monopulse antenna and comparator network with transparent layers, (b) monopulse antenna and network arrangement for X band.

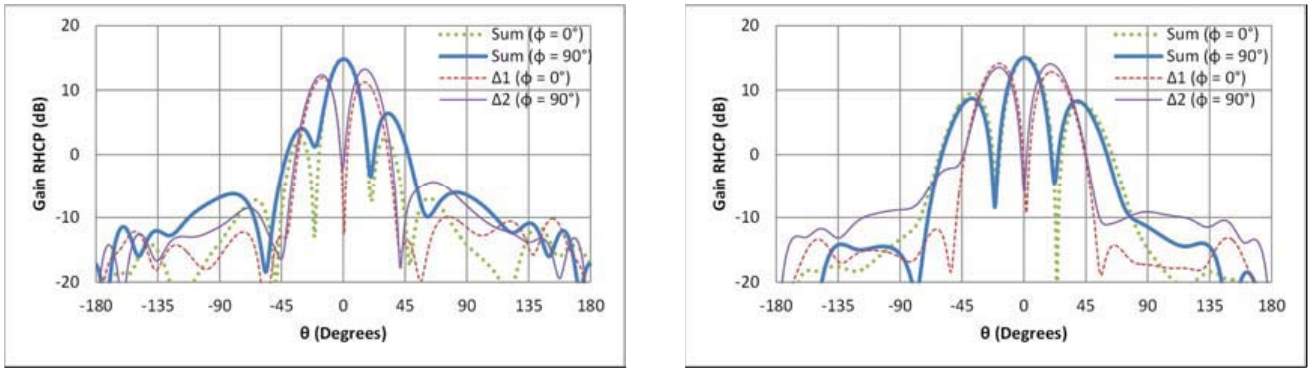

(a) (b)

Figure 5. Simulated radiation pattern using HFSS; RHCP gain of (a) the X band at 8.2 GHz and (b) the S band at 2.25 GHz.

RHCP gain and null depth are at least 15 dB for both frequency bands. Beam width is narrower, and side lobe level (SLL) is better for the X band antenna since it uses 2×2 array for each section instead of one patch as explained before.

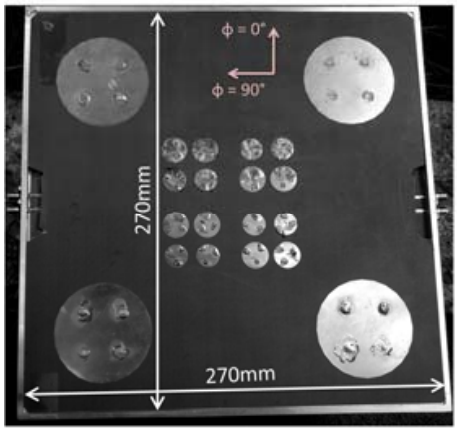

Figure 6. Photograph of the monopulse antenna.

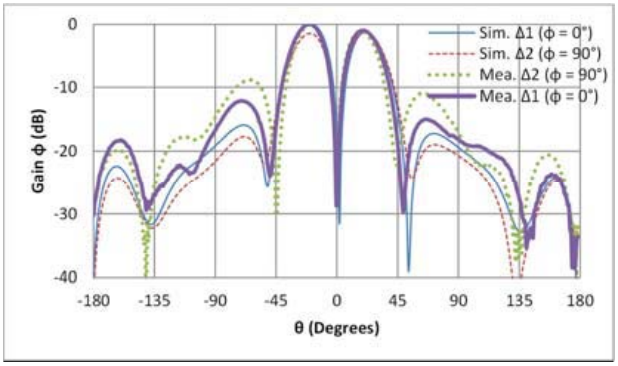

(a)

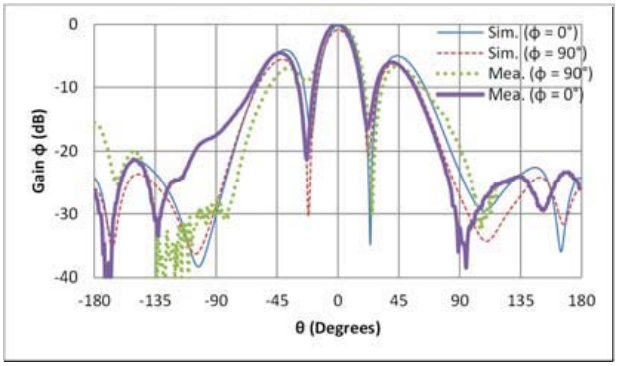

(b)

Figure 7. Simulated and measured radiation patterns of the S band at 2.25 GHz; Gain ϕ with the excitation at (a) the difference ports and (b) the sum port.

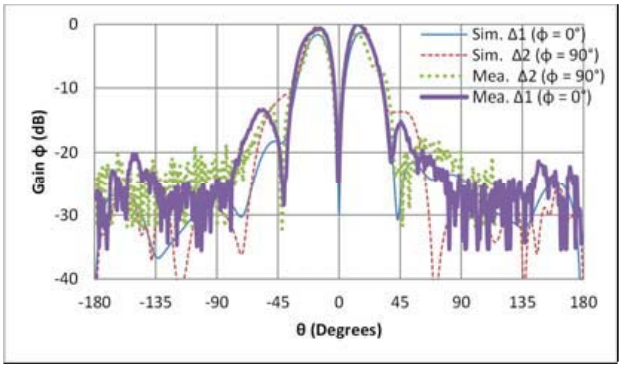

(a)

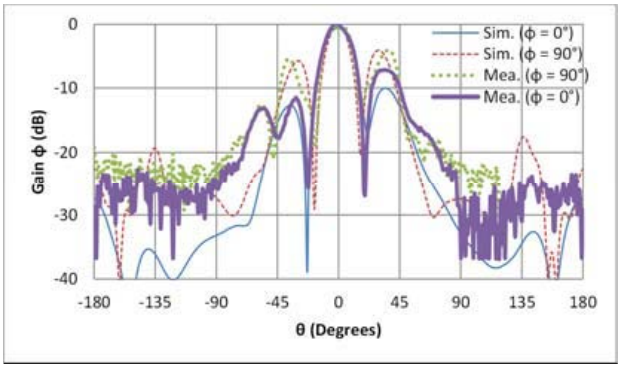

(b)

Figure 8. Simulated and measured radiation patterns of the X band at 8.2 GHz; Gain ϕ with the excitation at (a) the difference ports and (b) the sum port.

The fabrication method is as simple as what mentioned in [30] for one antenna, except that one should regard the collocation for each substrate. The realized antenna is shown in Fig. 6, and the radiation patterns of the S band antenna for the excitation at different inputs are compared with the simulation results in Fig. 7. Therefore, the monopulse antenna is assumed as the transmitter, and a vertically polarized antenna is used as a receiver for both $\phi = 0°$ and $\phi = 90°$ patterns. The monopulse antenna is placed so that the $\phi = 90°$ arrow stands vertical plane and that the $\phi = 0°$ arrow is turned in the horizontal plane for the $\phi = 0°$ patterns. Obviously the arrows are swapped for the $\phi = 90°$ patterns. Consequently, the gain in ϕ direction is obtained in both situations. It is seen that in these patterns null depth is further than 25 dB while the SLL decreases. It is possible to improve the SLL using larger arrays or adding absorbent walls around the antenna; however it is not necessary for our design since the side lobes are outside the spatial angle of the reflector. Similar results are shown for the X band antenna in Fig. 8. It indicates an almost good agreement between measured and simulated results except the SLLs of some radiation patterns which are higher than what is expected. A good evidence for the sameness of the phase center is the process of radiation pattern measurement, since it is performed without repositioning the antenna.

A distinction for this antenna is the wide bandwidth for both frequency bands. Simulated and measured reflections and axial ratio of the X band antenna are given in Fig. 9. It can be seen that the limitations of bandwidths are from the reflections because the axial ratio is less than 3 dB wherever the return loss is more than 10 dB. Therefore, the bandwidth is 12.7% in simulation and 10% in measurement for the X band antenna. It should be considered that the reflection of the Q port, which is shown by $P4$ in Fig. 4, is not assumed in the bandwidth calculation, since it will not be used in the monopulse system. Similar results are provided for the S band antenna in Fig. 10 as well as the axial ratio without the copper sheet. It can be observed that the axial ratio of this structure does not reduce to 7 dB without the copper sheet. In addition, the bandwidth is 10.2% in simulation and 10.3% in measurement for this frequency band. We observe in Fig. 10(c) that the reflections of some ports are smaller than what we have expected. It is due to the solders between serial feeds and probes that decrease the discontinuity and improve the performance uncontrollably. Some important characteristics of the antenna for the reflector application are given in Table 1.

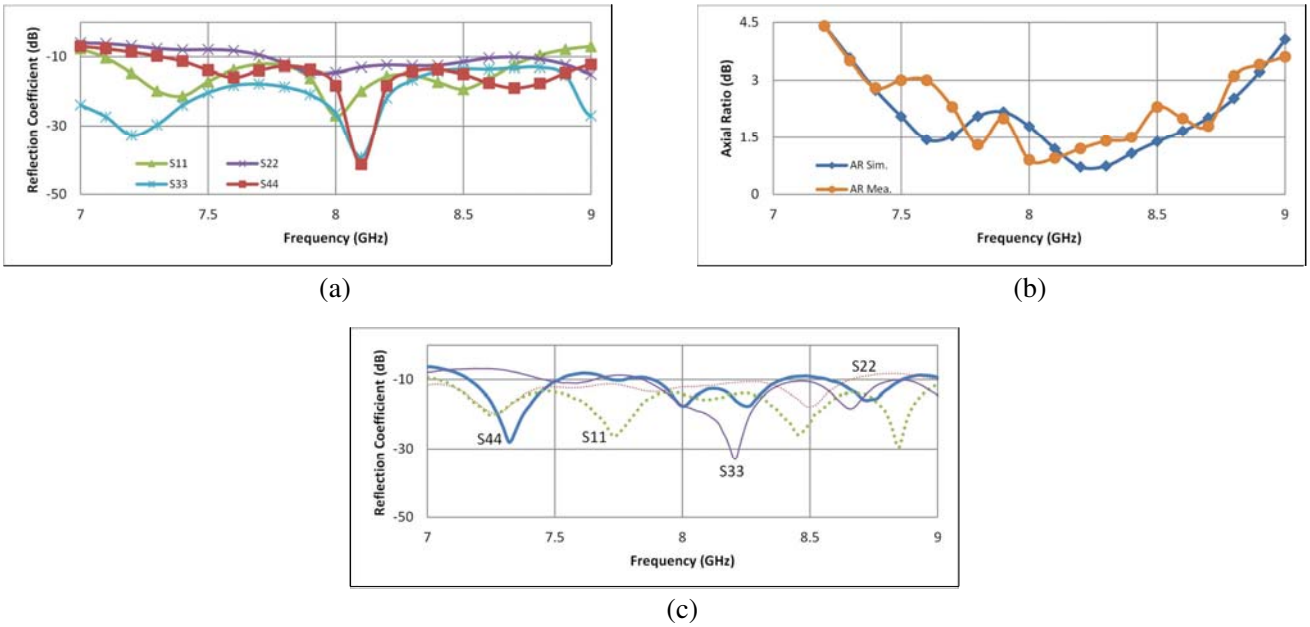

Figure 9. Simulated and measured results for X band, (a) simulated reflections, (b) axial ratio and (c) measured reflections.

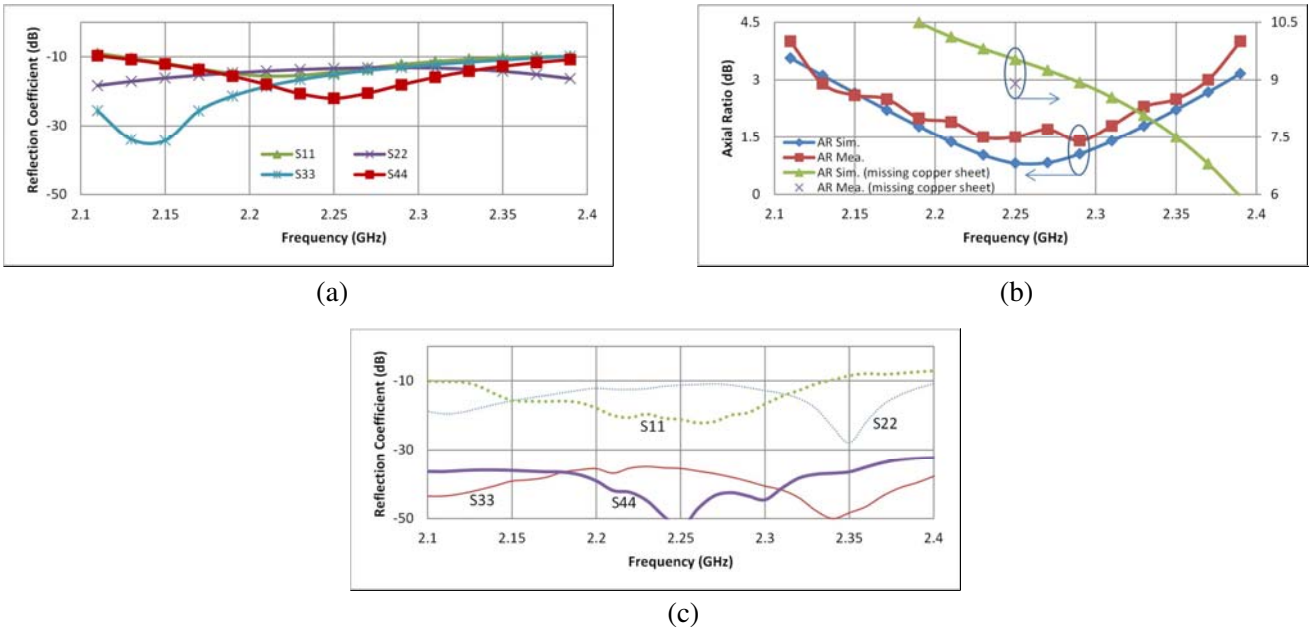

Figure 10. Simulated and measured results for S band, (a) simulated reflections, (b) axial ratio and (c) measured reflections.

Table 1. Characteristics of the antenna.

Frequency band	Gain (dB)	10 dB beam-width	Null depth CP (dB)	Null depth LP Sim. (dB)	Null depth LP Mea. (dB)
S	15.2	31°	20	31	28
X	15	30°	16	29	25
Frequency band	AR BW Sim. (%)	AR BW Mea. (%)	S_{11} BW Sim. (%)	S_{11} BW Mea. (%)	-
S	11	10.8	11.1	10.7	-
X	18.2	17.3	12.7	10	-

4. CONCLUSIONS

This paper presents the design and realization of circularly polarized dual-band monopulse antenna with unique phase center that can be used as a feed for a reflector antenna. The antennas are designed separately for each frequency band and placed on a substrate in the vicinity of each other, and the feed networks are placed separately on different layers. The coupling effect for the S band antenna is compensated using a copper sheet bellow the X band feed network. The design presented in this paper has been efficiently applied as a feed antenna for remote sensing earth station and has been validated experimentally. Good agreement between simulated and experimental results is observed, and a bandwidth of more than 10% for each frequency band has been achieved. This method can cover any desired dual-frequency-bands with enough distance.

REFERENCES

1. Skolnik, M. I. (ed.), *Radar Handbook*, McGraw-Hill, New York, 1970.
2. Nystrom, G. L., "Synthesis of broad-band 3-dB hybrids based on the 2-way power divider," *IEEE Trans. Microw. Theory Tech.*, Vol. 29, No. 3, 189–194, Mar. 1981.

3. Fartookzadeh, M., S. H. Mohseni Armaki, and M. Kazerooni, "A novel 180° hybrid based on the modified Gysel power divider," *Progress In Electromagnetics Research C*, Vol. 27, 209–222, 2012.
4. Arigong, B., J. Shao, M. Zhou, J. Ding, H. S. Kim, and H. Zhang, "A novel dual-band rat-race coupler," *IEEE Wireless and Microwave Technology Conference (WAMICON)*, 2014.
5. Marcus Oliver, J., P. Ralston, E. Cullens, L. Ranzanic, K. Vanhille, and S. Raman, "A W-band micro coaxial passive monopulse comparator network with integrated cavity-backed patch antenna array," *2011 IEEE MTT-S International Microwave Symposium Digest (MTT)*, 2011.
6. Wang, H., D. G. Fang, and X. G. Chen, "A compact single layer monopulse microstrip antenna array," *IEEE Trans. Microw. Theory Tech.*, Vol. 54, No. 2, 503–509, Feb. 2006.
7. Liu, B., W. Hong, Z. Kuai, X. Yin, G. Luo, J. Chen, H. Tang, and K. Wu, "Substrate integrated waveguide (SIW) monopulse slot antenna array," *IEEE Transactions on Antennas and Propagation*, Vol. 57, No. 1, 275, 2009.
8. Masa-Campos, J. L. and P. Rodriguez-Fernandez, "Monopulse circularly polarized SIW slot array antenna in millimetre band," *Journal of Electromagnetic Waves and Applications*, Vol. 25, Nos. 5–6, 857–868, 2011.
9. Subbarao, B. and V. Fusco, "Probe-fed circularly polarised monopulse radial line slot antenna," *Electronics Letters*, Vol. 39, No. 21, 1495–1496, 2003.
10. Kumar, Ch., V. S. Kumar, and V. V. Srinivasan, "Design aspects of a compact dual band feed using dielectric rod antennas with multiple element monopulse tracking," *IEEE Transactions on Antennas and Propagation*, Vol. 61, No. 10, Oct. 2013.
11. Nasimuddin, K. Esselle, and A. K. Verma, "Compact circularly polarized enhanced gain microstrip antenna on high permittivity substrate," *Proc. IEEE Asia-Pacific Conf., APMC 2005*, Vol. 4, 2005.
12. Ferrero, F., C. Luxey, G. Jacquemod, and R. Staraj, "Dual-band circularly polarized microstrip antenna for satellite applications," *IEEE Antennas Wireless Propag. Lett.*, Vol. 4, No. 1, 13–15, 2005.
13. Zhou, Y., C. C. Chen, and J. L. Volakis, "Single-fed circularly polarized antenna element with reduced coupling for GPS arrays," *IEEE Transactions on Antennas and Propagation*, Vol. 56, No. 5, 1469–1472, 2008.
14. Bernard, L., G. Chertier, and R. Sauleau, "Wideband circularly polarized patch antennas on reactive impedance substrates," *IEEE Antennas Wireless Propag. Lett.*, Vol. 9, 359–362, 2010.
15. Khidre, A., K. F. Lee, F. Yang, and A. Elsherbeni, "Wideband circularly polarized E-shaped patch antenna for wireless applications," *IEEE Antennas and Propagation Magazine*, Vol. 52, No. 5, 219–319, 2010.
16. Wu, Z. H., Y. Lou, and E. K. Yung, "A circular patch fed by a switch line balun with printed L-probes for broadband CP performance," *IEEE Antennas Wireless Propag. Lett.*, Vol. 6, 608–611, 2007.
17. Guo, Y. X., K. W. Khoo, and L. C. Ong, "Wideband circularly polarized patch antenna using broadband baluns," *IEEE Transactions on Antennas and Propagation*, Vol. 56, No. 2, 319–326, 2008.
18. Lin, C., F.-S. Zhang, Y.-C. Jiao, F. Zhang, and X. Xue, "A three-fed microstrip antenna for wideband circular polarization," *IEEE Antennas Wireless Propag. Lett.*, Vol. 9, 359–362, 2010.
19. Lo, W. K., C. H. Chan, and K. M. Luk, "Bandwidth enhancement of circularly polarized microstrip patch antenna using multiple L-shaped probe feeds," *Microw. Opt. Technol. Lett.*, Vol. 42, No. 4, 263–265, 2004.
20. Huang, J., "C.P. microstrip array with wide axial ratio bandwidth and single feed L.P. elements," *IEEE Antennas Propag. Soc. Int. Symp. Dig.*, 705–708, 1985.
21. Teshirogi, T., M. Tanaka, and W. Chujo, "Wide-band circularly polarized array antenna with sequential rotations and phase shift of elements," *Int. Symp. Antennas Propagat., ISAP*, 117–120, Tokyo, Japan, 1985.
22. Chung, D. C., C. H. Yun, K. H. An, S. H. Lim, S. Y. Choi, B. S. Han, J. H. Oh, M. H. Kwak, S. H. Jung, K. Y. Kang, S. K. Han, J. S. Hwang, T. H. Sung, and H. S. Choi, "HTS microstrip

antenna array for circular polarization with cryostat," *IEEE Trans. Appl. Supercond.*, Vol. 15, No. 2, 1048–1051, 2005.

23. Nasimuddin, Z. N. Chen, and K. P. Esselle, "Wideband circularly polarized microstrip antenna array using a new single feed network," *Microw. Opt. Technol. Lett.*, Vol. 50, No. 7, 1784–1789, 2008.
24. Hung, K. F. and Y. C. Lin, "Broadband printed circularly-polarised aperture antenna array for millimetre-wave gigabit applications," *Electronics Lett.*, Vol. 44, No. 25, 1439–1441, 2008.
25. Weng, C. H., H. W. Liu, C. H. Ku, and C. F. Yang, "Dual circular polarisation microstrip array antenna for WLAN/WiMAX applications," *Electronics Lett.*, Vol. 46, No. 9, 609–611, 2010.
26. Shahabadi, M., D. Busuioc, A. Borji, and S. Safavi-Naeini, "Low-cost, high-efficiency quasi-planar array of waveguide-fed circularly polarized microstrip antennas," *IEEE Transactions on Antennas and Propagation*, Vol. 53, No. 6, 2036–2043, 2005.
27. Evans, H., P. Gale, B. Aljibouri, E. G. Lim, E. Korolkciwicz, and A. Sambel, "Application of simulated annealing to design of serial feed sequentially rotated 2×2 antenna array," *Electronics Lett.*, Vol. 36, 1987–1988, 2000.
28. Jazi, M. N. and M. N. Azarmanesh, "Design and implementation of circularly polarized microstrip antenna array using a new serial feed sequentially rotated technique," *Inst. Elect. Eng. Proc. Microw. Antennas Propag.*, Vol. 153, No. 2, 133–140, 2006.
29. Chen, A., Y. Zhang, Z. Chen, and C. Yang, "Development of a Ka-band wideband circularly polarized 64-element microstrip antenna array with double application of the sequential rotation feeding technique," *IEEE Transactions on Antennas and Propagation*, Vol. 10, 1270–1273, 2011.
30. Gao, S., Y. Qin, and A. Sambell, "Low-cost broadband circularly polarized printed antennas and array," *IEEE Antennas Propag. Mag.*, Vol. 49, No. 4, 57–64, 2007.
31. Bilotti, F. and C. Vegni, "Design of high-performing microstrip receiving GPS antennas with multiple feeds," *IEEE Antennas and Wireless Propag. Lett.*, Vol. 9, 248–251, 2010.
32. Fartookzadeh, M. and S. H. Mohseni Armaki, "Serial-feed for a circular patch antenna with circular polarization suitable for arrays," *International Journal of RF and Microwave Computer-Aided Engineering*, Vol. 24, No. 5, 529–535, 2014.